

Convex Formulations of Aggregate Network Air Traffic Flow Optimization Problems

Daniel B. Work, *Student Member, IEEE*, Alexandre M. Bayen, *Member, IEEE*

Abstract—The problem of regulating air traffic in the en route airspace of the National Airspace System is studied using an Eulerian network model to describe air traffic flow. The evolution of traffic on each edge of the network is modeled by a modified Lighthill-Whitham-Richards partial differential equation. We pose the problem of optimal traffic flow regulation as a continuous optimization program in which the partial differential equation appears in the constraints. The equation is transformed with a variable change which removes the nonlinearity in the control variables and enables us to use linear finite difference schemes to discretize the problem. Corresponding linear programming and quadratic programming based solutions to this convex optimization program yield a globally optimal solution. The technique is applied for a network scenario in the Oakland Air Route Traffic Control Center.

I. INTRODUCTION

Research on the steady increase in air traffic volume has triggered the development of a new class of *aggregate* flow models, which describe the evolution of flows of aircraft rather than individual trajectories in the hope of capturing traffic patterns in a tractable manner. To our best knowledge, the article [1] was the first to define traffic flow using an *Eulerian*, or control volume based, framework based on a discretized version of the *Lighthill-Whitham-Richards* (LWR) *partial differential equation* (PDE) [2], [3]. This work has since inspired several research groups to generate similar models using a stochastic framework [4], [5]. Two dimensional models [6] have also emerged, in the hope of capturing traffic flow patterns more precisely. An important characteristic of these approaches [1], [4], [5], [6] is the diffusion or dispersion that they exhibit.

A first attempt to resolve these issues was proposed in the form of a continuous time - continuous space model in earlier work of one of the authors [7], based directly on the LWR PDE. While this approach solves the diffusion problem, its corresponding optimization programs require heavy computations based on adjoint problems. In the work [8], the authors compare the predictive capabilities of the *Large Capacity Cell Transmission Model* (CTM(L)) proposed in [9] with three other Eulerian models, and highlight the computational issues with the PDE model which motivate the present article. This work addresses the suboptimality problem faced in [7] by using a new convex formulation of the same problem, which also improves the computational tractability of the model significantly with respect to previous continuous approaches such as [8].

One of the most powerful techniques used for solving problems posed as optimization programs in which con-

straints appear in the form of PDEs is adjoint-based optimization [10]. This framework is very general, and enables systematic treatment of cost functions and constraints. This method has two main drawbacks: (i) it does not provide any guarantee of global optimality for non-convex problems; (ii) it is computationally expensive, due to the necessity of sequentially solving a series of “direct” and “adjoint” problems and using iterative descent methods such as the *Broyden-Fletcher-Goldfarb-Shanno* (BFGS) method to optimize the cost [11].

The present article addresses these two problems by formulating the problem as a convex optimization problem, which provides a globally optimal solution to the problem posed earlier in [7], at a lower computational cost (one *linear* or *quadratic program* (LP or QP) vs. an adjoint optimization procedure).

The remainder of this work is organized as follows. In section II we describe the PDE network model which is used as a constraint in subsequent optimization problems. We show the optimization problem can be transformed into a convex program, which allows us to efficiently solve for globally optimal solutions, which is a key contribution of this work. We discretize the convex problem to solve it numerically and discuss the potential pitfalls which can occur when selecting a numerical scheme in section III. In section IV we apply the method to a trajectory tracking problem under reduced network capacity on the Oakland Air Route Traffic Control Center.

II. PROBLEM FORMULATION

A. PDE Network Model

This section uses the PDE model of air traffic flow initiated in [7], and later extended in [8]. This approach models jetways as paths composed of a series of line segments known as links. We represent each link k on a path as a segment $[0, L]$ and denote by $u(x, t)$ the number of aircraft between distances 0 and x at time t . We can define the density of aircraft as the weak derivative of $u(x, t)$ with respect to x : $\rho(x, t) = \frac{\partial u(x, t)}{\partial x}$. The aircraft density is a solution of the partial differential equation:

$$\begin{cases} \frac{\partial \rho(x, t)}{\partial t} + v(x, t) \frac{\partial \rho(x, t)}{\partial x} + \frac{\partial v(x, t)}{\partial x} \rho(x, t) = 0, & (x, t) \in (0, L) \times (0, T) \\ \rho(x, 0) = \rho_0(x), & x \in [0, L] \\ \rho(0, t) = \frac{q_0(t)}{v(0, t)}, & t \in [0, T] \end{cases} \quad (1)$$

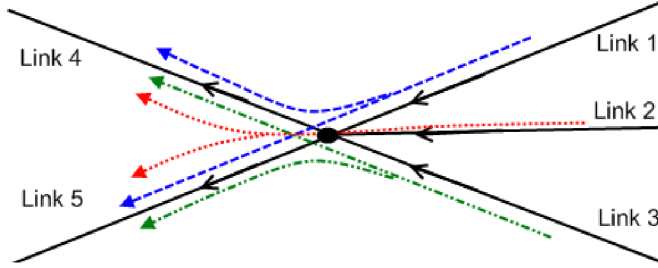


Figure 1. Simple example network composed of five links. The flow from links 1 (dashed), 2 (dotted), and 3 (dash dot) each split and feed links 4 and 5.

This PDE is a linear advection equation with positive velocity and a source term: $\frac{\partial v(x,t)}{\partial x} \rho(x,t)$. Note that while equation (1) is linear in the state $\rho(x,t)$, if $v(x,t)$ is also introduced as an unknown parameter to be determined by the optimization program, then (1) becomes nonlinear when considered as a constraint.

This model of air traffic flow on a link can be extended to a network of links. We let \mathbb{K} denote the set of all links in the network. For each link $k \in \mathbb{K}$ we associate the set \mathbb{M}_k with the set of all links in the network in which flow merges into link k . We represent the portion of flow exiting link $m \in \mathbb{M}_k$ which enters link k by $\beta_{m,k}$, where $0 \leq \beta_{m,k} \leq 1$. Because flow exiting m may split onto multiple links including k , we require that for a fixed m , $\sum_{i \in \mathbb{K}} \beta_{m,i} = 1$. That is, the flow exiting from link m and diverging to all other links i must be conserved. For the simple network shown in Fig. 1, we have $\mathbb{K} := \{1, \dots, 5\}$, $\mathbb{M}_4 = \mathbb{M}_5 = \{1, 2, 3\}$ and $\beta_{m,4} + \beta_{m,5} = 1$, $m \in \{1, 2, 3\}$.

The system of partial differential equations on a general network can be written as:

$$\begin{cases} \frac{\partial \rho_k(x,t)}{\partial t} + v_k(x,t) \frac{\partial \rho_k(x,t)}{\partial x} + \frac{\partial v_k(x,t)}{\partial x} \rho_k(x,t) = 0, \\ (x,t) \in (0, L_k) \times (0, T], k \in \mathbb{K} \\ \rho_k(x,0) = \rho_{0,k}(x), x \in [0, L_k], k \in \mathbb{K} \\ \rho_k(0,t) = \frac{q_{0,k}(t)}{v_k(0,t)} + \frac{\sum_{m \in \mathbb{M}_k} \beta_{m,k} \rho_m(L_m,t) v(L_m,t)}{v_k(0,t)}, \\ t \in [0, T], k \in \mathbb{K} \end{cases} \quad (2)$$

The well posedness of problem (2), and the existence and uniqueness of the solution on the network are proved in [8].

B. Optimal Control Problem

We now pose the problems of maximizing the aircraft arrivals at airports in the network, and optimal trajectory tracking in the en route and arrival airspace as optimal control problems. In other words, we seek to find the globally optimal velocity profiles $v_k(x,t)$ with respect to some network performance metric, for all links in the system.

1) *Objective Functions:* In order to pose the objective functions, we introduce a single airport α , in the set of all airports \mathbb{A} in the network. If we wish to denote the number of arrivals of aircraft at airport α through time t by $\eta_\alpha(t)$, we can maximize the total number of arrivals by forming the

following objective function: $\min J = -\sum_{\alpha \in \mathbb{A}} \eta_\alpha(T)$. If we let a link terminating at airport α be denoted by k_α , then k_α belongs to the subset of links terminating at one of the airports in the set of all airports defined by $\mathbb{K}_\mathbb{A} \subseteq \mathbb{K}$. We note that the integral $\int_0^t q_{k_\alpha}(L_{k_\alpha}, s) ds$ represents the cumulative arrivals $\eta_\alpha(t)$ at airport α at time t , and so this objective can be implemented in terms of the PDE model variables (with $q(x,t) = \rho(x,t)v(x,t)$) as:

$$\min J = -\sum_{k_\alpha \in \mathbb{K}_\mathbb{A}} \int_0^T q_{k_\alpha}(L_{k_\alpha}, t) dt \quad (3)$$

Note that this objective function is linear in q . With a proper (linear) discretization in space and time, it will lead to a linear program when subject to linear constraints.

We introduce a quadratic control objective, namely trajectory tracking by matching the desired flight plans as closely as possible. This is accomplished by first computing the desired density and flux distributions $\rho_{k,\text{des}}(x,t)$ and $q_{k,\text{des}}(x,t)$ corresponding to the desired flight plans of all aircraft in the network. In practice, this is a useful formulation when some unforeseen event, such as inclement weather, reduces the capacity of the network and forces deviations from the desired schedule. We formalize this objective as:

$$\min J = \sum_{k \in \mathbb{K}} \int_0^T \int_0^{L_k} \left((q_k(x_k,t) - q_{k,\text{des}}(x_k,t))^2 + (\rho_k(x_k,t) - \rho_{k,\text{des}}(x_k,t))^2 \right) dx_k dt \quad (4)$$

We note that a third control objective can also be implemented as a quadratic program in this framework, namely to match a desired arrival schedule at all airports as closely as possible [12].

2) *Constraints:* Following standard optimal control terminology, we encode the dynamics of the system in the form of constraints [13]. The key constraint in the optimization program is thus the constitutive model equation given in the form of PDEs of the $\rho_k(x,t)$ functions. This also includes a prescribed initial density distribution $\rho_{0,k}(x,t)$, which represents the aircraft initially airborne. The inflow conditions at the boundaries of each link $q_{0,k}(t)$ correspond to aircraft entering the network, either from international flights or lower altitude traffic. We impose upper and lower bounds on the velocity profile on each link, $v_{k,\min}(x,t) \leq v_k(x,t) \leq v_{k,\max}(x,t)$, to keep traffic flow consistent with the physical capabilities of the aircraft in the NAS.

An upper bound on the density on each link $\rho_k(x,t) \leq \rho_{k,\max}(x,t)$ is added to capture the essence of a minimum horizontal separation distance between aircraft in the aggregated form, following the work on capacity constraints in the field of Eulerian models [1], [4], [5], [6], [7], [8], [12], [14], [15]. We also require the density to be non-negative to be physically meaningful.

3) *Transformation of the Problem into a Convex Optimization Program:* The key contribution of this article is

the transformation of a known problem [7], [8], [16] into a convex problem, a feature which was previously unknown. If the previously mentioned constraints are imposed along with the network PDE model, the optimization program for a single junction becomes:

$$\begin{aligned} \min_{\rho_k(x,t), v_k(x,t)} J \\ \text{s.t. } 0 \leq \rho_k(x,t) \leq \rho_{k,\max}(x,t) \\ v_{k,\min}(x,t) \leq v_k(x,t) \leq v_{k,\max}(x,t) \quad (5) \\ (x,t) \in [0, L_k] \times [0, T], \quad k \in \mathbb{K} \\ \text{system (2)} \end{aligned}$$

The goal of the optimization problem is to find the optimal $\rho(x,t)$ and $v_k(x,t)$ such that the objective function J is minimized. The output of this program is thus an optimal speed control policy to be applied by the air traffic controller. The principle difficulty with solving (5) is that the PDE is a nonlinear constraint in the optimization variables. Thus, even if linear discretization schemes are used, the resulting constraints will be nonlinear. We now propose a change of decision variables which makes the previous constraints in (5) linear:

$$q_k(x,t) = \rho_k(x,t)v_k(x,t) \quad (6)$$

The nonlinear constraint in terms of decision variables $\rho_k(x,t)$ and $v_k(x,t)$ can be transformed into a linear constraint in terms decision variables $\rho_k(x,t)$ and $q_k(x,t)$. The control variable $v_k(x,t)$ is completely absent in the resulting formulation, and so it must be computed from the optimal solutions for density and flux obtained by solving the following equivalent problem:

$$\begin{aligned} \min_{\rho_k(x,t), q_k(x,t)} J \\ \text{s.t. } 0 \leq \rho_k(x,t) \leq \rho_{\max}(x,t) \\ v_{k,\min}(x,t)\rho_k(x,t) \leq q_k(x,t) \\ \leq v_{k,\max}(x,t)\rho_k(x,t) \\ \frac{\partial \rho_k(x,t)}{\partial t} + \frac{\partial q_k(x,t)}{\partial x} = 0 \quad (7) \\ \rho_k(x,0) - \rho_{0,k}(x) = 0 \\ q_k(0,t) - q_{0,k}(t) \\ - \sum_{m \in \mathbb{M}_k} \beta_{m,k} q_m(L_m, t) = 0 \\ (x,t) \in [0, L_k] \times [0, T], \quad k \in \mathbb{K} \end{aligned}$$

Note also that the velocity constraint changed from bounds on $v_k(x,t)$ in (5) to a linear constraint on $q_k(x,t)$ and $\rho_k(x,t)$ in (7). In this latter form, any linear discretization scheme will yield a discrete formulation which can be solved numerically using either linear or quadratic programming techniques, depending on the objective function and its discretization. This formulation, (both continuous and discrete) is the main contribution of the article, and was previously unknown.

III. PRACTICAL IMPLEMENTATION

A. Description of Discretization Schemes

1) *Notation:* For each link in the network, we must discretize the continuous variables into their discrete forms. Dropping the link subscript k for brevity, the physical domain for $\rho(x,t)$ and $q(x,t)$ with $(x,t) \in [0, L] \times [0, T]$ is written in terms of the discrete variables ρ_i^n and q_i^n where i and n are integers in $[0, i_{\max}]$ and $[0, n_{\max}]$ respectively, where $i_{\max} + 1$ and $n_{\max} + 1$ correspond to the number of discretization points in space and time. Letting $\lfloor \cdot \rfloor$ denote the floor operator, we define i in terms of the continuous space x and the discrete space step size Δx , as: $i = \lfloor \frac{x}{\Delta x} \rfloor$, and note that $i_{\max} + 1$ corresponds to the number of discretization points in the space domain. Similarly, n is defined in terms of the continuous time variable t and the discrete time step size ΔT , as: $n = \lfloor \frac{t}{\Delta T} \rfloor$, and $n_{\max} + 1$ equals the number of discretization points in time.

2) *Schemes Implemented:* A variety of discretization schemes applied to the the modified LWR PDE constraint (7) have been tested for use in this optimization framework, and we now present a subset to illustrate key challenges. The (explicit) *Lax-Friedrichs* (LxF) scheme is written in terms of $\rho(x,t)$ and $q(x,t)$ following [17]:

$$\rho_i^{n+1} = \frac{1}{2}(\rho_{i+1}^n + \rho_{i-1}^n) - \frac{1}{2} \frac{\Delta T}{\Delta x} (q_{i+1}^n - q_{i-1}^n) \quad (8)$$

which is subject to the *Courant-Friedrichs-Lewy* (CFL) condition: $|\frac{\Delta T}{\Delta x} v_i^n| \leq 1$ for stability [17]. Since v_i^n is an unknown optimization variable, we must insure stability for all possible v_i^n , namely: $|\frac{\Delta T}{\Delta x} v_{\max}| \leq 1$. Alternatively, if a second order centered difference in space at the t and $t + 1$ time steps are averaged, the (implicit) *Crank-Nicholson* (CN) scheme is obtained [18]:

$$\rho_i^{n+1} = \rho_i^n - \frac{\Delta T}{4\Delta x} (q_{i+1}^{n+1} - q_{i-1}^{n+1} + q_{i+1}^n - q_{i-1}^n) \quad (9)$$

We also present the (implicit) *Crank-Nicholson with dissipation* (CND) scheme [17]:

$$\rho_i^{n+1} = \rho_i^n - \frac{\Delta T}{4\Delta x} (q_{i+1}^{n+1} - q_{i-1}^{n+1} + q_{i+1}^n - q_{i-1}^n) - \frac{\varepsilon}{16} (q_{i+2}^n - 4q_{i+1}^n + 6q_i^n - 4q_{i-1}^n + q_{i-2}^n) \quad (10)$$

which has a dissipative term of order 4 for small values of ε (i.e. $\varepsilon = \frac{1}{2}$). An upcoming journal version of this article contains additional schemes and a comparison of their computation time and accuracy [19].

3) *Boundary Conditions:* When implementing any numerical scheme, special attention must be paid to boundary conditions. In this optimization program, we implement the boundary conditions in the strong sense, at the first grid point in the physical domain because it is an inflow condition. Downstream, we implement boundary conditions with ghost points, following the procedure outlined in [8], [20]. This is now presented on the LxF scheme, while noting that a similar procedure is used on the other schemes.

The initial distribution of density on each link k , given by $\rho_{0,k}(x)$ is directly imposed in the discrete problem as follows: $\rho_{i,k}^0 = \rho_{0,k}(i\Delta x)$. If the initial velocity profile $v_{0,k}(x)$ at the initial time is also known, the initial flux profile can be defined similarly: $q_{i,k}^0 = \rho_{0,k}(i\Delta x)v_0(i\Delta x)$.

At the link entrance, we impose the inflow flux on link k on the discrete flux variable $q_{0,k}^n$ according to:

$$q_{0,k}^n = q_{0,k}(n\Delta T) + \sum_{m \in \mathbb{M}_k} \beta_{m,k} q_m(i_{\max}\Delta x, n\Delta T) \quad (11)$$

This expression can be interpreted as follows: The discrete flux variable $q_{0,k}^n$ on each link k , at the boundary $i = 0$, is equal to the inflow flux function $q_{0,k}(t)$ representing all aircraft entering the network at link k , plus the fluxes from all links which feed flow already in the network into link k . The density along the link entrance $\rho_{0,k}^n$ is bounded but not specified directly at this boundary; its optimal value is computed directly from the optimization program.

With variables now defined along the initial time and space boundaries, the LxF scheme (8) is encoded as a constraint involving $\rho_i^n, \rho_{i+1}^n, \rho_{i-1}^n, q_{i+1}^n$, and q_{i-1}^n for all $i \in [1, i_{\max}]$ and $n \in [1, n_{\max}]$. Because ρ_{i+1}^n and q_{i+1}^n are undefined in the PDE evaluation at i_{\max} , we introduce a ghost point at $i_{\max} + 1$ which is not in the physical domain. Instead, it is used for the sole purpose of computing the flux and density variables at the link exit according to the discretized PDE constraint. These variables are constrained to the physical system by invoking the constraints:

$$\rho_{i_{\max}+1}^n = \rho_i^n, \quad q_{i_{\max}+1}^n = q_i^n \quad (12)$$

B. Computational Results

We now discuss two common pitfalls when implementing the discretization schemes through the following example. Specifying the boundary condition on the inflows:

$$q_0^n = \begin{cases} 0 & \text{for } n\Delta T \leq \frac{1}{4} \\ \sin(2\pi(1 - 2n\Delta T)) & \text{for } n\Delta T \in [\frac{1}{4}, \frac{1}{2}] \\ 0 & \text{for } n\Delta T \geq \frac{1}{2} \end{cases} \quad (13)$$

and initial density distribution:

$$\rho_i^0 = \begin{cases} \sin(2\pi i\Delta x) & \text{for } i\Delta x \in [0, \frac{1}{2}] \\ 0 & \text{for } i\Delta x \in [\frac{1}{2}, 2] \end{cases} \quad (14)$$

we solve the following discretized maximization of airport arrivals *validation problem* on a single link subject to a bump inflow condition and initial density distribution, for one link with the LxF scheme. We define:

$$v_{i,\max}^n = v_{i,\min}^n = \begin{cases} 2 & \text{for } i\Delta x \in [0, 1] \\ 3 - i\Delta x & \text{for } i\Delta x \in [1, 2] \end{cases} \quad (15)$$

and the validation problem is given by:

$$\begin{aligned} \min_{\rho_i^n, q_i^n} & - \sum_{n=0}^{n_{\max}} q_{i_{\max}}^n \Delta T \\ \text{s.t. } & \rho_i^{n+1} = \frac{1}{2}(\rho_{i+1}^n + \rho_{i-1}^n) - \frac{1}{2} \frac{\Delta T}{\Delta x} (q_{i+1}^n - q_{i-1}^n) \\ & \rho_{i_{\max}}^{n+1} = \frac{1}{2}(\rho_{i_{\max}}^n + \rho_{i_{\max}-1}^n) \\ & \quad - \frac{1}{2} \frac{\Delta T}{\Delta x} (q_{i_{\max}}^n - q_{i_{\max}-1}^n) \\ & -\frac{1}{5} \leq \rho_i^n \leq 3 \\ & \rho_i^n v_{i,\min}^n \leq q_i^n \leq \rho_i^n v_{i,\max}^n \\ & i \in [1, i_{\max}], \quad n \in [1, n_{\max}] \end{aligned} \quad (16)$$

eqn. (13)

eqn. (14)

Note that the second constraint represents the discretized PDE with the ghost points correctly implemented at the link exit boundary. As revealed by our study, while problem (7) or its discrete counterpart (16) is convex in theory, a simple implementation of these programs which does not take into account specific features of the numerical schemes often results in (numerical) infeasibility or meaningless solutions. This occurs even when physically meaningful solutions exist for the continuous programs.

1) *Infeasibility*: One ironic feature of the numerical implementation is the fact that a problem can become infeasible by relaxing the velocity constraint from $v_{\min}(x, t) = v_{\max}(x, t)$ to $v_{\min}(x, t) < v_{\max}(x, t)$: seemingly increasing the feasible set of valid velocities results in infeasibility! This is the case for the CND scheme. To see why this occurs, we examine the second constraint in the formulation (7): $v_{\min}(x, t)\rho(x, t) \leq q(x, t) \leq v_{\max}(x, t)\rho(x, t)$. In the framework of air traffic control, the density and flux should remain non-negative to be physically meaningful. However, the discrete formulations of the LWR PDE can introduce an overshoot which causes the density to become slightly negative (see Fig. (2)). In the problem formulation, we can relax the explicit constraint that $\rho(x, t) \geq \rho_{\min}$ (with $\rho_{\min} = 0$) to accommodate this numerical error. In the validation problem, this causes a proportional negative flux, but the problem remains feasible (assuming it does not violate the relaxed ρ_{\min} constraint). The same can not be said for the control problem. Even when the ρ_{\min} constraint is relaxed to allow for overshoot, the problem formulation has an implicit constraint that $\rho(x, t) \geq 0$. To see why, we assume $\rho(x, t) \leq 0$, and note that the constraint on q would become:

$$v_{\min}(x, t) \cdot (-1)|\rho(x, t)| \leq q(x, t) \leq v_{\max}(x, t) \cdot (-1)|\rho(x, t)| \quad (17)$$

which leads to the following contradiction:

$$v_{\min}(x, t) \geq v_{\max}(x, t) \quad (18)$$

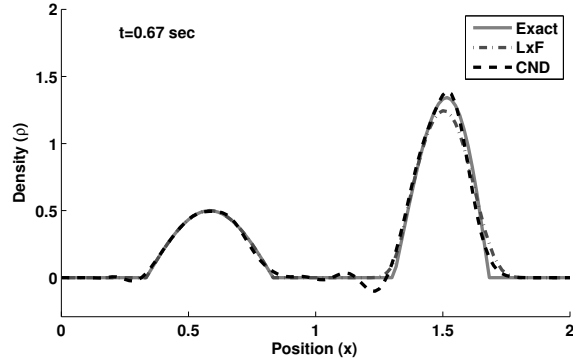


Figure 2. Comparison of the computed density LxF and CN schemes and the exact solution to problem (16) at time $t = 0.67$ seconds. Vertical axis density (ρ). Horizontal axis: position (x). The LxF scheme is feasible for the control problem, while the CN scheme is infeasible, because of the undershoot clearly visible, which violates $\rho(x, t) \geq 0$ locally due to numerical inaccuracy.

Thus, schemes such as CN, which are very accurate overall for the validation problem, cannot be used for the control problem because of a slight negative overshoot (see Fig. 2) making the optimization program infeasible.

2) *Physically Meaningless Solutions*: Another implementation challenge occurs when implicit schemes such as CN are used in the optimization framework of (7). Although these schemes are unconditionally stable, they may still suffer from significant sawtooth-like oscillations, as shown in Fig. 3. This figure shows the result of solving a control problem with constant initial and boundary conditions. The observed oscillations are a direct consequence of the symmetric centered spatial difference of $\frac{\partial q(x, t)}{\partial x}$ that appears in (9). This symmetry opens the potential for solutions to the discretized PDE which are not solutions to its continuous counterpart. For example, consider the original PDE constraint: $\frac{\partial \rho(x, t)}{\partial t} + \frac{\partial q(x, t)}{\partial x} = 0$, and impose an additional constraint that $\frac{\partial \rho(x, t)}{\partial t} = 0$ for all x and all t . In the continuous framework, any solution to the optimization problem with this constraint must necessarily satisfy $\frac{\partial q(x, t)}{\partial x} = 0$. Taking the discrete version of this condition by applying a centered difference operator on the spatial derivative of q , we find there are multiple solutions to the discretized constraint $\frac{q_{i+1}^n - q_{i-1}^n}{2\Delta x} = 0$. One such solution, corresponding to the analytic solution of the continuous constraint is:

$$q_0^n = q_1^n = \dots = q_{i_{\max}}^n = C \quad (19)$$

where C is a constant. A more pathological solution to the difference equation can be expressed as:

$$\begin{cases} q_1^n = q_3^n = q_5^n = \dots = C_1 \\ q_0^n = q_2^n = q_4^n = \dots = C_2 \end{cases} \quad (20)$$

where C_1 and C_2 are constants. Here, the spatial profile of the flux oscillates between the values of C_1 and C_2 , and therefore would not satisfy the continuous constraint in the

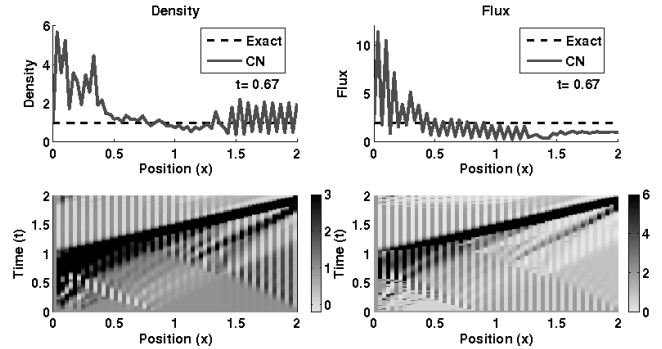


Figure 3. Density (left column) and flux (right column) solutions to a control problem with constant boundary and initial conditions: $q(0, t) = 2$, $\rho(x, 0) = 1$, with $v_{\min} = 0.5$ and $v_{\max} = 0.2$, at time $t = 0.67$ (top row). Surface plots of the density and flux (bottom row) show the solution exhibits oscillatory behavior. Color darkens with increasing density and flux.

limit: $\frac{\partial q}{\partial x} = 0$. On the other hand, it does satisfy the discrete constraints:

$$\begin{cases} \left(\frac{\partial q}{\partial x} \right)_{i=2} = \frac{q_3 - q_1}{2\Delta x} = \frac{C_1 - C_1}{2\Delta x} = 0 \\ \left(\frac{\partial q}{\partial x} \right)_{i=3} = \frac{q_4 - q_2}{2\Delta x} = \frac{C_2 - C_2}{2\Delta x} = 0 \end{cases} \quad (21)$$

Thus, this solution exists only in the discrete representation of the problem, and does not correspond to the physics of air traffic flows on the network.

Clearly, discrete models using the central difference operator have a potential for solutions with large deviations from the continuous model because they allow too much freedom for the solution to oscillate. The pathological cases presented in this section unfortunately happen frequently in practice, and thus require careful selection of a good numerical scheme which avoids the two pitfalls presented in sections III-B2 and III-B1.

IV. APPLICATION TO THE OAKLAND AIR ROUTE TRAFFIC CONTROL CENTER

A. Model Construction

Using previous modeling work (see [8], [9]), we now apply the proposed algorithm to the en route and arrival airspace in the Oakland Center, which we have studied in the past and for which we have a database of *Aircraft Situation Display to Industry* (ASDI) data. In [8], we have validated a model of en route traffic flow against this data and assessed its accuracy. The selected subset of this network, depicted in Fig. 4, consists of 14 links merging into the Oakland *Terminal Radar Approach Control* (TRACON), in which traffic follows a 15th link. Corresponding historical velocity profiles $v(x)$ can be identified from the database. We construct this range from the historical mean, from which we allow speed amendments of $\pm 15\%$.

B. Flow Simulation

In the simulation presented next, 117 aircraft enter the network at the boundaries of 9 different links over a 6 hour

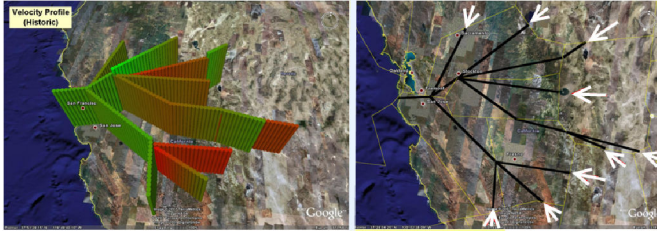


Figure 4. (left) Aggregate velocity profiles for each of the 15 links generated from actual flights on Jan. 1, 2005, with increasing height corresponding to increasing velocity. The leftmost link corresponds to the Oakland TRACON. (right) The network consists of links converging towards Oakland. Links with incoming inflows are denoted with arrows.

window shown in Fig. 4 (right). We convert each entering aircraft into a flux q used in the LWR PDE. Assuming the i^{th} aircraft enters link k at time t_i^k , it generates a flux $q_{k,i}(0, t)$ on the link over a time window z , according to the following:

$$q_{k,i}(0, t) = \begin{cases} \sin\left(\frac{t - (t_i^k - \frac{z}{2})}{z}\pi\right) & \text{if } t \in [t_i^k - \frac{z}{2}, t_i^k + \frac{z}{2}] \\ 0 & \text{Otherwise.} \end{cases} \quad (22)$$

The link flux boundary condition $q_k(0, t)$ is then obtained by summing the flux contributions over all aircraft entering the link $q_k(0, t) = \sum_i q_{k,i}(0, t)$. With velocity profiles obtained from the flights on Jan. 1 2005, and the inflow boundary conditions given by (4), we run the forward simulation to check the validity of the model using the LxF discretization scheme. The computations are performed with the LxF scheme in 4 seconds on a standard laptop running CPLEX, assuming a discrete spatial step of 4 nautical miles, and a discrete time step of 31 seconds, resulting in 357,072 variables. The corresponding results in Fig. 5 (left) show a sharp density increase (7 aircraft on a link) at the edges of the links nearest to the Oakland TRACON, which is a direct result of the merge geometry of the network.

C. Network Optimization Under Reduced Capacity

We now consider a scenario in which the capacity of each link in the network is reduced to 66% of the capacity under the nominal conditions. This decrease in capacity may have several causes, for example outgoing traffic, special use airspace, and weather disturbances. Although the capacity on a given portion of the network may be reduced, our objective is to minimize the effect of this capacity decrease on traffic through the network. In other words, we wish to find the optimal velocity control strategies for each link in the network which satisfies the reduced capacity constraint, and which track the full capacity trajectories as closely as possible. This objective is formally stated as (4), where $q_{k,des}^n$ and $\rho_{k,des}^n$ are the flux and density obtained from the unconstrained forward simulation.

In order to meet the reduced capacity constraint, we allow the velocity profiles to increase or decrease by at most 15%

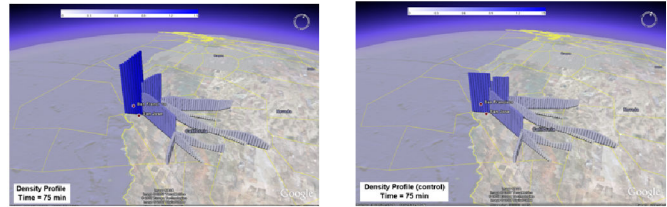


Figure 5. Results Showing the evolution of density on the network operating at full capacity (left) and at a capacity reduced to 66% (right) from time 75 minutes. Increasing height and darkening color indicates the increasing density on the links.

from the historical average on each link. The quadratic optimization problem runs in 45 seconds on average, outperforming adjoint-based methods [8] on earlier formulations by at least one order of magnitude for speed of computation, with the added benefit of providing a globally optimal solution to the problem. Thus, for a given set of inflows into the network, a forward simulation, and optimization to find a solution meeting a reduced capacity constraint can be completed in less than a minute on a standard laptop for the entire arrival airspace shown in the right column of Fig. 4. The globally optimal changes to the density evolution caused by a 33% reduction in the capacity are displayed in Fig. 5 for $t = 75$ min, in which the height on each link corresponds to the magnitude of the density. Because of the certificate of global optimality, and because the resulting objective is positive definite [21], this is the unique globally optimal solution which minimizes changes to the flight schedule.

The striking feature of the reduced capacity simulations are that minimal changes to the aircraft density upstream can lead to significant changes in the link downstream. Furthermore, we can examine the schedule of aircraft exiting the network under full and reduced capacity in Fig. 6. The peaks in the full capacity simulation correspond to times when a large number of aircraft is arriving simultaneously into the Oakland TRACON. The valleys show periods when fewer aircraft are arriving into the TRACON. As a result of the reduced capacity, the desired arrival schedules of all aircraft cannot be met at the peak time. Instead, the aircraft arrival times must be more evenly distributed in time, as shown in Fig. 6. The benefit of the optimization framework developed in this work is that the changes to the flight plans are the global minimum which satisfy the reduced capacity constraints.

V. CONCLUSION

The fundamental contribution of this article is the formulation of a classical partial differential equation-based optimal control problem (maximization of throughput in a network or minimization of delays) as a convex program (either quadratic or linear in the present case). This is a significant improvement over previous techniques based on adjoint optimization which are computationally an order of magnitude more demanding and do not provide guarantees of optimality. This article also displayed two nontrivial pitfalls underlining the fact that “posing a problem as a convex

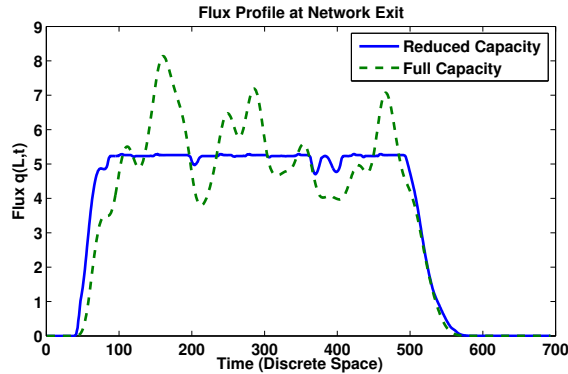


Figure 6. Comparison of the flux profile (vertical axis) at the last point in the network, for the unconstrained (dotted) network, and the network with capacity reduced to 66% (solid).

optimization program” does not provide a systematic solution to engineering problems. In particular, without an appropriate choice of numerical scheme for the problem formulation, two things can happen: (i) overshoots or undershoots of numerical schemes (even if the schemes are very accurate) or (ii) systematically make optimization programs infeasible if some of the constraints are active where the overshoot happens.

ACKNOWLEDGMENT

We are grateful to Dr. Robin Raffard for sharing with us his assessment of the feasibility of posing the first problem outlined in this article as a convex program, based on an earlier conversation with Professor Claire Tomlin, Professor Anthony Jameson, and Professor Stephen Boyd. We want to thank Dengfeng Sun for his help with ASDI data, and for sharing his numerical database for this project.

REFERENCES

- [1] P. MENON, G. SWERIDUK, and K. BILIMORIA, “New approach for modeling, analysis, and control of air traffic flow,” *AIAA Journal of Guidance, Control, and Dynamics*, vol. 27, no. 5, pp. 737–744, 2004.
- [2] M. LIGHTHILL and G. WHITHAM, “On kinematic waves. II. A theory of traffic flow on long crowded roads,” *Proceedings of the Royal Society of London. Series A, Mathematical and Physical Sciences*, vol. 229, no. 1178, pp. 317–345, 1955.
- [3] P. I. RICHARDS, “Shock waves on the highway,” *Operations Research*, vol. 4, no. 1, pp. 42–51, 1956.
- [4] S. ROY, B. SRIDHAR, and G. C. VERGHESE, “An aggregate dynamic stochastic model for air traffic control,” in *Proceedings of the 5th USA/Europe ATM 2003 R&D Seminar*, (Budapest, Hungary), June 2003.
- [5] B. SRIDHAR, T. SONI, K. SHETH, and G. CHATTERJI, “An aggregate flow model for air traffic management,” in *AIAA Conference on Guidance, Navigation, and Control*, (Providence, RI), August 2004. AIAA Paper 2004–5316.
- [6] P. MENON, G. SWERIDUK, T. LAM, G. DIAZ, and K. BILIMORIA, “Computer-aided Eulerian air traffic flow modeling and predictive control,” *AIAA Journal of Guidance, Control, and Dynamics*, vol. 29, no. 1, pp. 12–19, 2006.
- [7] A. BAYEN, R. RAFFARD, and C. TOMLIN, “Adjoint-based control of a new Eulerian network model of air traffic flow,” *IEEE Transactions on Control Systems Technology*, vol. 14, no. 5, pp. 804–818, 2006.
- [8] D. SUN, I. STRUB, and A. BAYEN, “Comparison of the performance of four Eulerian network flow models for strategic air traffic flow management,” *Networks and Heterogeneous Media*, vol. 2, no. 4, pp. 569–594, 2007.
- [9] D. SUN and A. BAYEN, “A new Eulerian-Lagrangian large-capacity cell transmission model for en route traffic,” *AIAA Journal of Guidance, Control and Dynamics*, vol. 31, no. 3, pp. 616–628, 2008.
- [10] A. JAMESON, L. MARTINELLI, and N. PIERCE, “Optimum aerodynamic design using the navier-stokes equations,” *Theoretical and Computational Fluid Dynamics*, vol. 10, no. 1, pp. 213–237, 1998.
- [11] C. ZHU, R. BYRD, and J. NOCEDAL, “L-BFGS-B: Algorithm 778: L-BFGS-B, FORTRAN routines for large scale bound constrained optimization,” *ACM Transactions on Mathematical Software*, vol. 23, no. 4, pp. 550–560, 1997.
- [12] R. RAFFARD, S. WASLANDER, and C. TOMLIN, “Toward efficient and equitable distributed air traffic flow control,” in *Proceedings of the 2006 American Control Conference*, (Minneapolis, MN), pp. 5189–5194, June 2006.
- [13] F. BORRELLI, *Constrained Optimal Control of Linear & Hybrid Systems*, vol. 290 of *Lecture Notes in Control and Information Sciences*. Berlin, Germany: Springer Verlag, 2003.
- [14] A. BAYEN, P. GRIEDER, G. MEYER, and C. TOMLIN, “Lagrangian delay predictive model for sector-based air traffic flow,” *AIAA Journal of Guidance, Control, and Dynamics*, vol. 28, no. 5, pp. 1015–1026, 2005.
- [15] R. L. RAFFARD and C. J. TOMLIN, “Second order adjoint-based optimization of ordinary and partial differential equations with application to air traffic flow,” in *Proceedings of the American Control Conference*, (Portland, OR), pp. 798–803, 2005.
- [16] R. RAFFARD, K. AMONLIRDVIMAN, J. AXELROD, and C. TOMLIN, “An adjoint-based parameter identification algorithm applied to planar cell polarity signaling,” *IEEE Transactions on Automatic Control Special Issue on Systems Biology*, vol. 53, pp. 109–121, January 2008.
- [17] C. HIRSCH, *Numerical Computation of Internal & External Flows: Fundamentals of Numerical Discretization*. John Wiley & Sons, Inc. New York, NY, 1988.
- [18] J. C. STRIKWERDA, *Finite Difference Schemes and Partial Differential Equations*. Philadelphia, PA: SIAM, 2004.
- [19] D. WORK and A. M. BAYEN, “Convex formulations of aggregate network flow air traffic management problems.” To appear, *Proceedings of the IEEE Special Issue on Aviation Information Systems*.
- [20] I. STRUB and A. BAYEN, “Weak formulation of boundary conditions for scalar conservation laws: an application to highway modeling,” *International Journal on Robust and Nonlinear Control*, vol. 16, pp. 733–748, 2006.
- [21] S. BOYD and L. VANDENBERGHE, *Convex Optimization*. Cambridge, UK: Cambridge University Press, 2004.